ELSEVIER

Chemical Engineering Journal 141 (2008) 278–283

Chemical Engineering Journal

www.elsevier.com/locate/cej

Study on gas–liquid phase mass transfer coefficient of entrained flow reactor

Hu Lishun, Wang Xinjun, Yu Guangsuo *, Wang Fuchen, Yu Zunhong

Key Laboratory of Coal Gasification of Ministry of Education, Shanghai 200237, PR China

Received 29 August 2007; received in revised form 5 December 2007; accepted 28 December 2007

Abstract

The gas–liquid phase mass transfer coefficient of entrained flow reactor is studied in the paper. The liquid solvent is atomized into the entrained flow reactor after going through a type of pressure nozzle used in the experiment. The isometric decompression technique is used to investigate the mass transfer coefficient of the entrained flow reactor in seven different gas–liquid systems. The effect on mass transfer coefficient of *Re* and *We* number of droplet is sufficiently discussed. A mass transfer coefficient correlation model is proposed and the parameters in the model are obtained by nonlinear regression method. The residual shows that the model values are in good agreement with the experiment values.

Keywords: Entrained flow reactor; Gas–Liquid phase mass transfer coefficient; Pressure type nozzle; Atomization

1. Introduction

Entrained flow reactor has been used in chemical, petrochemical and biochemical processing [1–5], especially in coal gasification technology [6–12]. During last decades, the gasification process of an entrained flow gasifier has been widely investigated. Advantages of the entrained flow gasifier are the ability to utilize nearly any type of coals with high throughputs per reactor volume and the simpler mechanical design with nearly 100% carbon conversion. Koppers-Totzek, GE, Shell, Prenflo and GSP are well-known entrained flow coal gasification processes in the world [13–15].

Atomization and liquid residence time distribution in the entrained flow reactor has been widely investigated; flow pattern and mass transfer process are always neglected in previous work. Substantially, atomization is only a prerequisite condition to inter-phase mixture, flow pattern of entrained flow reactor brings reactant micelle mixture and the gas–liquid contact surface is increased sharply so as to enhance mass transfer in the entrained flow reactor.

Mass transfer coefficient of entrained flow reactor is studied in the paper. Considering the gas flux has little effect on the mass transfer in an entrained flow reactor as shown in reference [16], the effect of liquid flux on mass transfer is investigated emphatically. The nozzle used in the experiment is a type of pressure nozzle whose atomization theory is explained later. Mass transfer rate in the entrained flow reactor is obtained by isometric decompression technique.

2. Experimental

2.1. Experiment setup and procedures

The entrained flow reactor is a vertical column with 100 mm in inner diameter and 1.3 m in height. The liquid solvent is loaded in the liquid store tank (3), the pressure of which is provided by the nitrogen cylinder (1) and measured by a pressure gauge (2). The liquid solvent is atomized into the reactor after it goes through the nozzle (4) which is set on top of the entrained flow reactor (5). The pressure of the reactor is measured by a precision pressure gauge (7). All the experiments are carried out in normal temperature and atmosphere. The schematic of the overall experimental system is shown in Fig. 1.

A pressure type nozzle with double channels as shown in Fig. 2 is installed on the top of the reactor. The liquid solvent goes into a swirl chamber of center channel in tangent direction

* Corresponding author.
E-mail address: gsyu@ecust.edu.cn (G. Yu).

1385-8947/$ – see front matter © 2008 Elsevier B.V. All rights reserved.
doi:10.1016/j.cej.2007.12.032

Nomenclature

A	parameter
A_a	air core area (m^2)
A_o	outlet area of nozzle (m^2)
C_A^*	saturated concentration of gas in liquid (mol/m^3)
C_{Af}	gas concentration in liquid at outlet (mol/m^3)
ΔC_{Af}	mass transfer force of solute at outlet (mol/m^3)
C_{Ai}	gas concentration in liquid at inlet (mol/m^3)
ΔC_{Ai}	mass transfer force of solute at inlet (mol/m^3)
$\Delta C_{A,lm}$	average mass transfer force (mol/m^3)
C_D	discharge coefficient of nozzle
d_o	droplet diameter (m)
D	diffusion coefficient (m^2/s)
k_1	parameter
k_2, k_3	parameter
k_la	volumetric mass transfer coefficient (s^{-1})
m_L	mass flow rate (kg/s)
Δm	mass differential (kg)
M	molecular weight (g/mol)
ΔP	differential pressure (MPa)
Q_L	volumetric flow rate (m^3/s)
R	gas constant
Re	*Re* number
Sc	Schmidt number
Sh	Schwood number
t	mass transfer time (s)
T	temperature (K)
u	outlet velocity of droplet (m/s)
u_m	mass transfer rate (kg/s)
V	volume of reactor (m^3)
We	*We* number

Greek symbols

μ_i	*i*-component liquid viscosity (mPa s)
μ_L	paraffin viscosity (mPa s)
μ_m	mixture viscosity (mPa s)
ρ_A	gas density (kg/m^3)
ρ_L	paraffin density (kg/m^3)
σ_m	mixture surface tension (N m)
σ_o	solute surface tension (N m)
σ_w	water surface tension (N m)

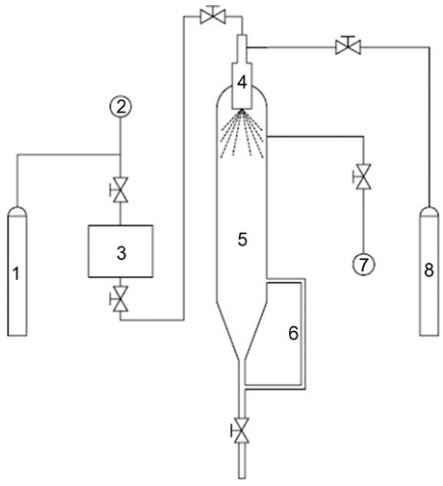

Fig. 1. Schematic of the overall experimental system. (1) Nitrogen cylinder, (2) pressure gauge, (3) liquid store tank, (4) pressure type nozzle, (5) entrained bed, (6) content gauge, (7) precision pressure gauge and (8) gas cylinder.

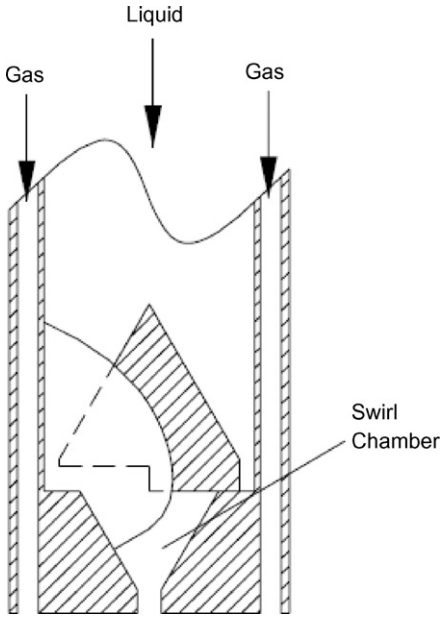

Fig. 2. Details of the pressure nozzle.

at a high speed and atomizes into the reactor from the outlet at the bottom of the nozzle.

2.2. Experiment procedure

The isometric decompression technique is used to measure mass transfer rate in an entrained flow reactor according to the following steps:

(1) Loading a known amount of liquid solvent into the liquid store tank, lifting the pressure of the tank by nitrogen till desirable value.
(2) Using gas solute to purge the reactor for a few minutes until the air in the reactor is all eliminated.
(3) Closing the bottom valve of the reactor, filling the reactor with amount of liquid solvent and recording the liquid level.
(4) Filling the reactor with some gas solute and writing down the pressure of reactor P_0 ($P_0 < 20{,}000$ Pa).
(5) Opening the forward valve of nozzle the liquid would be atomized into reactor, then closing the forward valve after a certain time and recording the time by a stopwatch.
(6) Opening the bottom valve of the reactor, discharging the liquid to the level recorded in (3), recording the pressure of reactor P_1.

Table 1
Experimental operating conditions

Gas	Liquid	Pressure drop (MPa)
CO_2	H_2O	0.3, 0.5, 0.8, 1.0, 1.2, 1.4
C_2H_2	H_2O	0.3, 0.5, 0.8, 1.0, 1.2, 1.4
O_2	H_2O	0.8, 1.0, 1.2, 1.4
CO_2	Paraffin	0.5, 0.8, 1.0, 1.2, 1.4
CO_2	*n*-Octane	0.3, 0.5, 0.8, 1.0, 1.2, 1.4
CO_2	Glycerol water solution*	0.3, 0.5, 0.8, 1.0, 1.2, 1.4
O_2	*n*-Hexane	0.3, 0.5, 0.8, 1.0, 1.2, 1.4

* 1:1 by volume.

2.3. Assumption

(1) The gas–liquid mass transfer only exists in the process of atomization, the mass transfer between the gas and still liquid is neglected.
(2) The experiment is carried out under normal temperature and atmosphere, so the gas is seemed as ideal gas, and the equilibrium between gas and liquid is conformed to Henry's law.
(3) The pressure in liquid store tank is much higher than the reactor and the pressure drop caused by the pipeline and liquid level is neglected, so the differential pressure of the nozzle could be regarded as the pressure in the liquid store tank.
(4) In the procedure of mass transfer, the pressure in the reactor is much lower than the atmosphere, so the mass transfer coefficient is obtained by Henry's law constant under normal atmosphere.

2.4. Experimental conditions and properties of solvent

Three kinds of gas solutes and five liquid solvents are used in the experiment. The gas–liquid mass transfer coefficient in the entrained flow reactor is obtained from 0.3 to 1.4 MPa. The details of operating conditions are listed in Table 1 and the properties of liquid solvent are shown in Table 2.

2.5. Relationship of differential pressure and flux of nozzle

In the procedure of atomization, the relationship of the liquid flux and differential pressure of nozzle is [20]:

$$m_L = C_D A_o (2\rho_L \Delta P)^{0.5} \tag{1}$$

where C_D is discharge coefficient of nozzle, the equation proposed by Giffen and Muraszew [21] is used to calculate C_D as follows:

$$C_D = 1.17 \left[\frac{(1-X)^3}{1+X} \right]^{0.5} \tag{2}$$

$$X = \frac{A_a}{A_o} \tag{3}$$

2.6. Droplet diameter

The liquid droplet diameter [22] after atomization in the experiment is in good agreement with Lefebvre's volume-surface average diameter [23] shown as follows:

$$d_o = 2.25\sigma^{0.25}\mu_L^{0.25} m_L^{0.25} \Delta P_L^{-0.5} \rho_A^{-0.25} \tag{4}$$

2.7. Mass transfer rate

Isometric decompression technique is used to determine the mass transfer rate in an entrained flow reactor. All the experiments are carried out in room temperature and atmosphere, based on the ideal gas equation:

$$\frac{P_1 - P_0}{t} V = \frac{\Delta m}{tM} RT \tag{5}$$

$$u_m = \frac{\Delta m}{t} = \frac{(P_1 - P_0)VM}{tRT} \tag{6}$$

2.8. Liquid volumetric mass transfer coefficient

For the gas–liquid mass transfer after atomization, the equation proposed by Tamir [24] is used to calculate the liquid volumetric mass transfer coefficient as follows:

$$Q_L(C_{Ai} - C_{Af}) = k_l A \Delta C_{A,lm} = k_l \alpha V \Delta C_{A,lm} \tag{7}$$

where $\Delta C_{A,lm}$ is determined by:

$$\Delta C_{A,lm} = \frac{\Delta C_{Ai} - \Delta C_{Af}}{\ln(\Delta C_{Ai}/\Delta C_{Af})} \tag{8}$$

$$\Delta C_{Ai} = C_A^* \tag{9}$$

$$\Delta C_{Af} = C_A^* - C_{Af} \tag{10}$$

3. Results and discussions

3.1. Differential pressure of nozzle

A type of pressure nozzle with double channels is used in the experiment. The liquid solvent goes into the swirl chamber of the center channel in tangent direction at a high speed. According to the conversation law of moment of momentum tangential speed is inversed ratio to swirl radius. At the outlet of the nozzle where liquid jets into reactor and atomizes with liquid static energy convert to kinetic energy as mentioned previously. Therefore, the differential pressure of nozzle has great effect on the droplet diameter after atomizing, as shown in Eq. (4) the differential pressure is inversed ratio to droplet diameter which means increasing the differential pressure of nozzle causes smaller droplet and increase in the interfacial surface between gas and liquid. It is shown from Fig. 3 that increase of differential pressure of nozzle promotes the mass transfer in an entrained flow reactor.

Table 2
Properties of liquid solvent used in the experiment

Component	Molecular weight (g/mol)	Density (kg/m^3)	Viscosity (mPa s)	Surface tension (mN/m)
Water	18.02	998	1.005	72.8
Glycerol	92.09	1261	1499	63
n-Octane	114.22	703	0.54	21.8
n-Hexane	86.17	659	0.313	18.2
Glycerol water solution*	–	1129.5	4.26[a]	66.26[b]
Paraffin	412	850.97[c]	15.19[d]	29.16[e]

All the properties are in standard state.
[a] Viscosity of mixture: $f(\mu_m)_L = \sum_i x_i f(\mu_i)_L$ [17].
[b] Tamura function: $\sigma_m^{1/4} = \varphi_W^{\sigma}\sigma_W^{1/4} + \varphi_0^{\sigma}\sigma_0^{1/4}$ [18].
[c] $\rho_L = 864.4 - 0.6714t$ [19].
[d] $\ln \mu_L = -3.0912 + 1.7038/T$ [19].
[e] $\sigma_L = 50.7657 \times 10^{-3} - 7.37 \times 10^{-5}T$ [19].
* 1:1 by volume.

3.2. Re number of droplet

Gas–liquid mass transfer takes place when the liquid solvent is atomized into entrained flow reactor. The gas–liquid mass transfer coefficient would be greatly affected by *Re* number of droplet, the definition of *Re* number of droplet is:

$$Re = \frac{d_o u \rho}{\mu} \tag{11}$$

Fig. 4 demonstrates that mass transfer coefficient in entrained flow reactor is promoted with *Re* number of droplet in seven gas–liquid systems, but in a certain gas–liquid system, *Re* number has not great change. There is no doubt that increasing differential pressure of nozzle brings small droplet with high-velocity, so significant change of *Re* number in a certain gas–liquid system should not be expected. However, the gas–liquid interface gets strong disturbance with the increase of *Re* number and small droplet augments gas–liquid mass transfer surface.

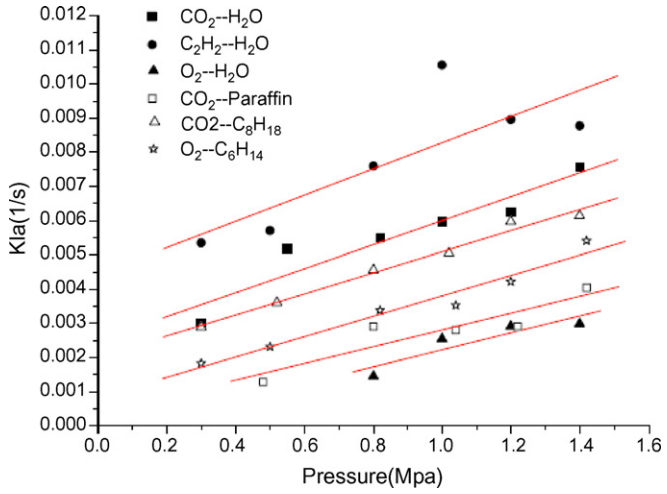

Fig. 3. Effect of pressure drop on K_1a.

3.3. We number of droplet

We number of droplet is ratio of droplet kinetic energy to surface energy. Breakup of droplet is affected by kinetic energy, surface energy and viscosity of liquid. To low viscosity liquid, the breakup of droplet is primarily determined by liquid kinetic energy and surface energy. *We* number of droplet is defined as follows:

$$We = \frac{\rho d_o u^2}{\sigma} \tag{12}$$

Lane [25] has shown experimentally that the mode of drop disintegration depends on whether the drop is subjected to steady acceleration or is suddenly exposed to a high-velocity gas stream. With steady acceleration the droplet becomes increasingly flattened, and at a critical relative velocity it is blown out into the form of a hollow bag attached to a roughly circular rim, the hollow bag break up into fine droplet when the *We* number reaches a critical value. It is shown from Fig. 5 that the mass transfer coefficient of entrained flow reactor is increased with *We* number of droplet. Distortion and breakup of droplet becomes strong when the *We* number increases and enhancement of the inner distribution of droplet leads to fluxion of solute from surface to inner of droplet. Consequently, mass transfer resistance at droplet surface is decreased.

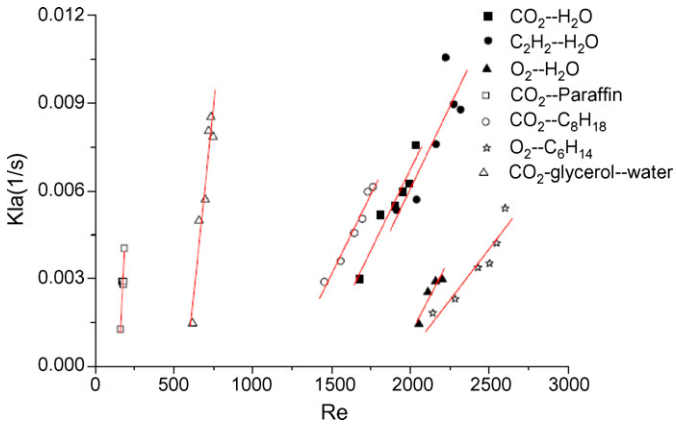

Fig. 4. Effect of *Re* number on K_1a.

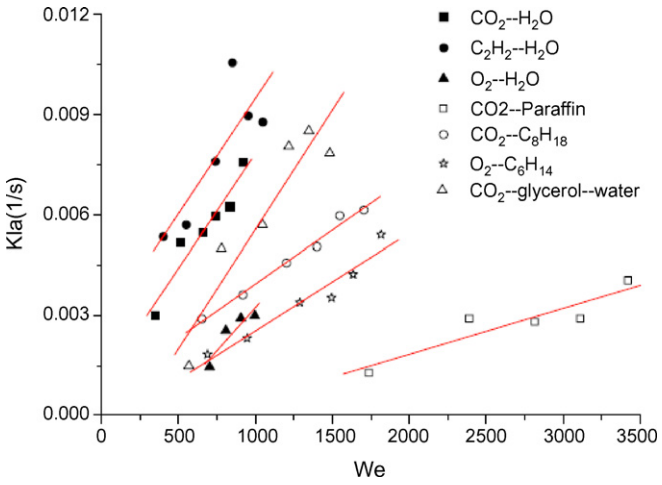

Fig. 5. Effect of *We* number on K_1a.

3.4. Mass transfer coefficient correlation

The liquid mass transfer coefficient of entrained flow reactor is correlated with liquid droplet velocity, droplet diameter, properties of gas and liquid and diffusion coefficient. Therefore, the liquid volumetric mass transfer coefficient could be shown as:

$$k_1a = f(d, u, \rho, \mu, \sigma, D)$$

change into mathematic model, there is:

$$Sh = A Re^{k_1} Sc^{k_2} We^{k_3}$$

where, A, k_1, k_2, k_3 are parameters fitted by nonlinear regression method.

$$Sh = 1.2889 \times 10^{-9} Re^{1.6617} Sc^{1.3914} We^{-0.7172} \quad (13)$$

The residual of model is investigated as shown in Fig. 6. Comparison of model *Sh* number and experimental *Sh* number is shown in Fig. 7. The model relative error is 26.88. Comparing to the model reported in reference [24] which is used in carbon dioxide–water system, the new model has a wide application.

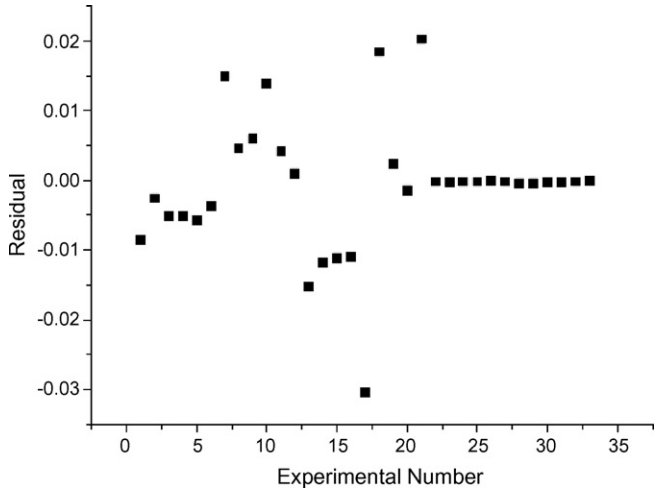

Fig. 6. The simulation residual of each experiment.

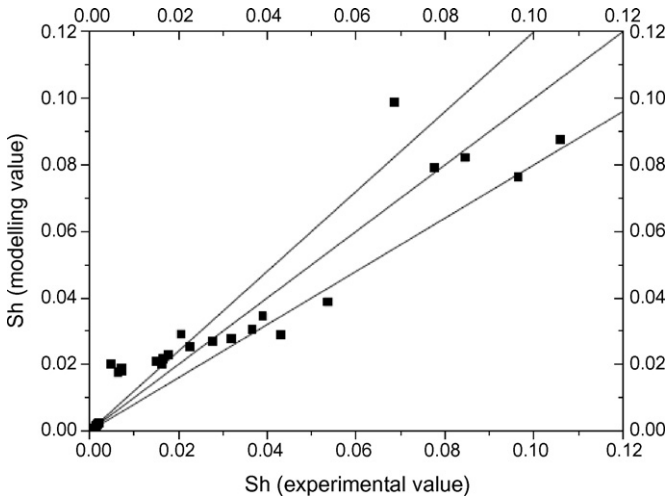

Fig. 7. Comparison of experimental *Sh* number and modeling *Sh* number.

4. Conclusion

The mass transfer in an entrained flow reactor has been studied in seven gas–liquid systems. Three gases and five liquids are used as solutes and solvents in the experiment, respectively. The experimental results declare that the increase of differential pressure of nozzle and improvement of *Re* and *We* number of droplet at outlet of nozzle promote the mass transfer coefficient of entrained flow reactor. Based on the experimental value, the correlation of liquid volumetric mass transfer coefficient of entrained flow reactor is obtained as:

$$Sh = 1.2889 \times 10^{-9} Re^{1.6617} Sc^{1.3914} We^{-0.7172}$$

References

[1] S. Xiu, W. Yi, Baoming Li, Flash pyrolysis of agricultural residues using a plasma heated laminar entrained flow reactor, Biomass Bioenergy 29 (2005) 135–141.
[2] J. Barroso, J. Ballester, L.M. Ferrer, S. Jimenez, Study of coal ash deposition in an entrained flow reactor: influence of coal type, blend composition and operating conditions, Fuel Process. Technol. 87 (2006) 737–752.
[3] E. Biagini, M. cioni, L. Tognotti, Development and characterization of a lab-scale entrained flow reactor for testing biomass fuels, Fuel 84 (2005) 1524–1534.
[4] D. Vamvuka, Modeling of an entrained flow coal gasifier. 2. Effect of operating conditions on reactor performance, Fuel 74 (10) (1995) 1461–1465.
[5] Z. Ye, C.J. Zygarlicke, K.C. Galbreath, J.S. Thompson, M.J. Holmes, J.H. Pavlish, Kinetic transformation of mercury in coal combustion flue gas in a bench-scale entrained-flow reactor, Fuel Process. Technol. 85 (2004) 463–472.
[6] J.G. Lee, Characteristics of entrained flow coal gasification in a drop tube reactor, Fuel 75 (9) (1996) 1035–1042.
[7] Xiaolei Guo, Zhenghua Dai, Xin Gong, Xueli Chen, Haifeng Liu, Fuchen Wang, Zunhong Yu, Performance of an entrained flow gasification technology of pulverized coal in pilot-scale plant, Fuel Process. Technol., in press.
[8] Miao Ren Niu, Qin Feng Liang, Guang Suo, Fu Chen Wang, Zun Hong Yu, Multifractal analysis of pressure fluctuation signals in an impinging entrained flow gasifier, Chem. Eng. Process., in press.
[9] H. Watanabe, M. Otaka, Numerical simulation of coal gasification in entrained flow coal gasifier, Fuel 85 (2006) 1935–1943.

[10] W. Vicente, S. Ochoa, J. Aguillon, E. Barrios, An Eulerian model for the simulation of an entrained flow coal gasifier, Appl. Therm. Eng. 23 (2003) 1993–2008.
[11] J. Faundez, Ignition behaviour of different rank coals in an entrained flow reactor, Fuel 84 (17) (2005) 2172–2177.
[12] G. Yu, Z. Zhou, Q. Qu, Z. Yu, Experimental studying and stochastic modeling of residence time distribution in jet-entrained gasifier, Chem. Eng. Process. 41 (2002) 595–600.
[13] M. Schingnitz, H. Brandt, F. Berger, P. Gohler, H. Kretschmer, Developments in the field of pressure gasification of pulverized brown coal in the German Democratic Republic, Fuel Process. Technol. 16 (3) (1987) 289–302.
[14] W.E.S. Preston, The Texaco Gasification Process in 2000 Startups and Objectives Presented at: 2000 Gasification Technologies Conference, San Francisco, CA, October 8–11, 2000.
[15] J.D. De Graaf, Q. Chen, D. Haag, An update on Shell Licensed Gasification Projects and Performance of Pernis IGCC Plant, Presented at: 2000 Gasification Technologies Conference, San Francisco, CA, 8–11 October 2000.
[16] A. Tamir, Impinging-stream Reactors—Fundamentals and Applications, Chemical Engineering Publisher, 1996, p. 272.
[17] J.S. Tong, Physical Property of Fluid, China Petrochemical Publisher, 1996, p. 250.
[18] J.S. Tong, Physical Property of Fluid, China Petrochemical Publisher, 1996, p. 339.
[19] B.C. Zhu, Chemical Reaction Engineering, third ed., Chemical Engineering Publisher, 2001, p. 336.
[20] A.H. Lefebvre, Atomization and Sprays, Hemisphere Publishing Corporation, 1987, p. 167.
[21] A.H. Lefebvre, Atomization and Sprays, Hemisphere Publishing Corporation, 1987, p. 168.
[22] Z.H. Yu, Study on Atomization and Residence Time Distribution in Complex Reactor [D], East China University of Science and Technology, 2006.
[23] A.H. Lefebvre, Atomization and Sprays, Hemisphere Publishing Corporation, 1987, p. 217.
[24] A. Tamir, Impinging-stream Reactors—Fundamentals and Applications, Chemical Engineering Publisher, 1996, pp. 277–279.
[25] W.R. Lane, Shatter of drops in streams of air, Ind. Eng. Chem. 43 (6) (1951) 1312–1317.